Prediction of Remarkably Large Second-Order Nonlinear Optical Properties of Organoimido-Substituted Hexamolybdates

Muhammad Ramzan Saeed Ashraf Janjua, Chun-Guan Liu, Wei Guan, Jia Zhuang, Shabbir Muhammad, Li-Kai Yan, and Zhong-Min Su*

Institute of Functional Material Chemistry, Faculty of Chemistry, Northeast Normal University, Changchun 130024, People's Republic of China

Received: October 1, 2008; Revised Manuscript Received: January 8, 2009

The dipole polarizabilities, dipole moments, density of states, and second-order nonlinear optical (NLO) properties of organoimido derivatives of hexamolybdates have been investigated by using time-dependent density functional response theory. This class of organic−inorganic hybrid compounds possesses remarkably large and eye-catching molecular second-order NLO response, especially $[Mo_6O_{17}(NC_{16}H_{12}NO_2)(FeNC_{10}H_9)]^{2-}$ (**7**) and $[Mo_6O_{17}(NC_{16}H_{12}NO_2)(NC_6H_2(NH_2)_3)]^{2-}$ (**6**) with static second-order polarizability (β_{vec}) computed to be 15766.27×10^{-30} esu and 6299.59×10^{-30} esu, respectively. Thus, these systems have the possibility to be excellent second-order nonlinear optical materials. Analysis of the major contributions to the β_{vec} value suggests that the charge transfer (CT) from polyanion to organic segment (D−A) along the *z*-axis plays the key role in NLO response; the polyanion acts as a donor (D) whereas organoimido acts as an acceptor (A) in all the studied systems. The computed β_{vec} values increase by incorporation of an electron acceptor ($-NO_2$) at the end of the phenyl ring of the organoimido segment. Furthermore, substitution of amino ($-NH_2$) or ferrocenyl ($-FeC_{10}H_9$) at the outer side of polyanion and an electron acceptor ($-NO_2$) at the end of the phenyl ring in organoimido segment simultaneously is more important to enhance the optical nonlinearity. Orbital analysis shows that the degree of CT between the polyanion and organoimido segments was increased when ferrocenyl donor was introduced. The present investigation provides important insight into the remarkably large NLO properties of organoimido-substituted hexamolybdates.

1. Introduction

Polyoxometalates (POMs) constitute a rich class of inorganic cluster systems and exhibit remarkable chemical and physical properties, which have been applied to a variety of fields, such as catalysis, medicine, biology, analytical chemistry, and materials science.[1−6] Recently, numerous novel POM functional materials have been synthesized. Among them, the POMs with covalently bonded organic species in their surfaces generate new multifunctional hybrid materials with fascinating structural, electrochemical, and photophysical properties, and this has become a focus of the synthesis chemistry of POMs.[7−13] In 1992, Judeinstein reported the first POM−polymer hybrid material in which a Keggin POM cluster was covalently linked to a polystyrene or polymethacrylate backbone through Si−O bonds.[14] Lalot and co-workers subsequently synthesized POM polymer cross-linked networks.[15−17] Stein and co-workers prepared macroporous silica materials with POM.[18,19] Maatta and co-workers reported organic polymers bearing polyoxometalates pendants.[20,21] The chemistry of POMs has gained great interest and led to promising applications. Among many organic derivatives of POMs, organoimido derivatives have attracted a particular interest. Lately, a large number of imido derivatives of the hexamolybdate anion have been synthesized continuously. Peng and co-workers prepared monofunctionalized, bifunctionalized, and dumbbell hybrid materials by means of a palladium-catalyzed coupling of a POM cluster with organoimido,[11,12,22,23] and they synthesized a high-purity disubstituted orthogonal hexamolybdate derivative by reacting α-$[Mo_8O_{26}]^{2-}$ with organoimido.[13] POMs have been found to be extremely versatile and multifarious inorganic building blocks for constructing the functionally active materials.[24] The covalent attachment of organic or organometallic groups to the POMs via linkages constitute an exceptionally interesting class of organic−inorganic hybrid polyoxoanions, It is noteworthy that such hybrid materials have been continuously and rapidly growing owing to their potential implementations in catalysis, medicine, magnetism, optics, conductivity, etc.[25,26]

Nonlinear optical processes are being increasingly actuated in a variety of optoelectronic and photonic applications. There subsist three generic categories of NLO material: semiconductors, inorganic salts, and organic compounds. Each category possesses its own complement of favorable and unfavorable attributes for NLO application.[27] Semiconductors possess NLO effects originating from saturable absorption.[28] Inorganic salts possess a large transparency range, are robust, are available as large single crystals, and suffer very low optical losses, but the purely electronic NLO effects are often accompanied by those arising from lattice distortions; response times are slow, and synchronization of the phase of the interacting optical fields is not easy to satisfy.[29] The organic materials are of major interest because of their relatively low cost, ease of fabrication and integration into devices, tailorability that allows one to fine-tune the chemical structure and properties for a given nonlinear optical process, high laser damage thresholds, low dielectric constants, fast nonlinear optical response times, and off-resonance nonlinear optical susceptibilities comparable to or exceeding those of ferroelectric inorganic crystals.[30] Organic materials have several disadvantages: low energy transitions in

* To whom correspondence should be addressed: e-mail, zmsu@nenu.edu.cn; phone, +86-431-85099108; fax, 86-431-85684009.

10.1021/jp808707q CCC: $40.75
Published on Web 03/19/2009

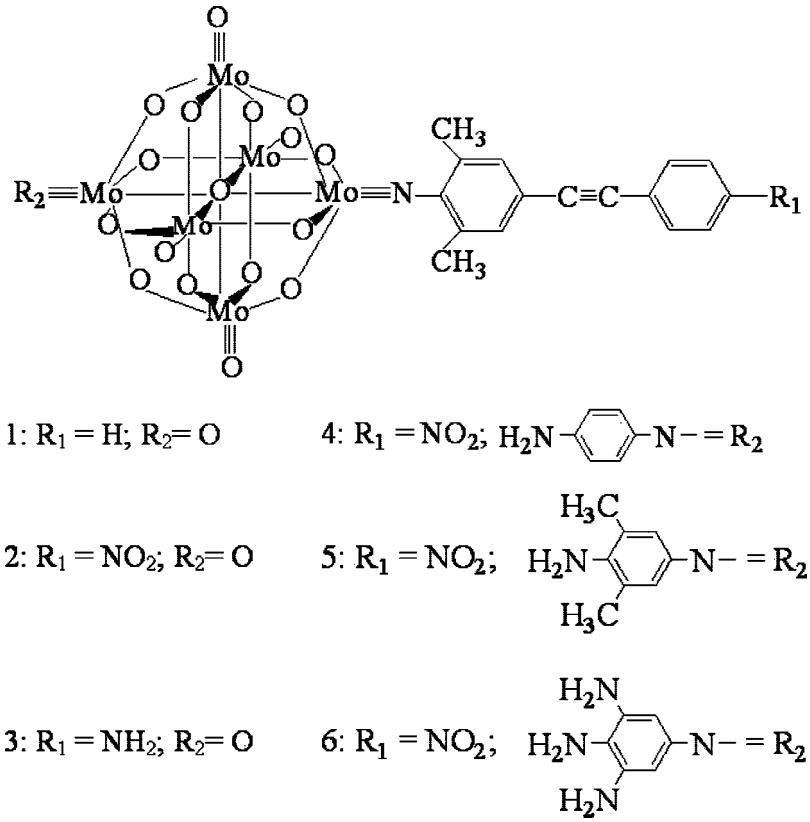

Figure 1. Calculation models for systems **1**−**6**.

the UV−vis region enhance the NLO efficiency but result in a tradeoff between nonlinear efficiency and optical transparency, they may have low thermal stability, and (in poled guest−host systems) they may undergo a facile relaxation to random orientation.[29] The circumscriptions identified above incite investigations of new materials. Among the many organic derivatives of POMs, organoidimide derivatives have been drawing increasing attention in that the strong d−π interaction between the organic delocalized π-electrons and the cluster d electrons may result in enchanting synergistic effects.[31] The bonding character between organoimido and $[Mo_6O_{19}]^{2-}$ has been studied by our group.[32] The results show that the strong Mo≡N triple bond can be formed, and this strong interaction generates a strong electronic communication between organoimido and $[Mo_6O_{19}]^{2-}$. That is, the intramolecular electron transfer can occur and results in large nonlinear optical response. Our theoretical study has also showed that those compounds have remarkable large second-order polarizability coefficients β.[33] Investigations have shown that nonlinear optical properties originate from the charge transfer of molecules. It has been reported that electron donor−acceptor compounds are potentially highly efficient NLO materials.[34] Considerable research efforts have been directed toward understanding the nature of the NLO phenomenon on organic compounds. Organic compounds consisting of push−pull molecules containing a donor and an acceptor connected via a conjugated bridge (D−π−A) have shown good NLO properties.[35]

Density functional theory (DFT) has become a significant tool for modeling the properties of molecules and materials. It therefore seems appealing to use DFT for the prediction of NLO properties as well.[36] DFT investigations on the POMs have made improvements.[37] Theoretical studies of NLO properties would be helpful in the rationalization of the observed properties of the POM system in itself and in the design of new, interesting POM-based molecular NLO materials. Our group has calculated a series of hexamolybdate complexes by using DFT,[33,38] and the results show that organoimido-to-hexamolybdates charge transfer was helpful to enhance the NLO responses of one-dimensional organoimido derivatives of hexamolybdates. However, the direction of charge transfer can be altered by changing the length of organic ligand. It is interesting that in our studied systems polyanion acts as a donor and organic ligand acts as an acceptor (D−A) which is different from other systems studied before.[33,38] Thus, in the present work we have designed different kinds of systems by incorporation of donors and acceptor; we performed DFT calculations on organoimido derivatives of hexamolybdates to predict their first hyperpolarizabilities. The effect on second-order polarizability is investigated by introducing an electron donor (−NH_2) or (−$FeC_{10}H_9$) at the outer side of polyanion and an electron acceptor (−NO_2) at the end of the phenyl ring simultaneously which established a donor−donor−acceptor−acceptor configuration (D−D−A−A). The structure−property relationship with organoimido POM derivatives will be helpful in designing the new NLO materials. This work may provide a useful means for designing high-performance nonlinear optical materials.

2. Computational Details

The DFT calculations were carried out using the ADF2006.01 suite of programs.[39] The zero-order regular approximation (ZORA) was adopted in all the calculations to account for the scalar relativistic effects.[40] The generalized-gradient approximation (GGA) was employed in the geometry optimizations by using the Beck[41] and Perdew[42] (BP86) exchange-correlation (XC) functional.

For the calculations, we made use of the standard ADF TZP basis set, which is triple-ζ plus polarization STO basis set.

TABLE 1: Bond Lengths (Å) and Angles (deg) Calculated by DFT for Systems 1−6

metrical parameters	1	2	3	4	5	6
C1−N1	1.349 (1.381)	1.337	1.349	1.335	1.335	1.334
Mo1−N1	1.814 (1.744)	1.829	1.810	1.822	1.825	1.822
Mo1−O1	2.240 (2.211)	2.245	2.258	2.297	2.297	2.288
N1−Mo1−O1	180 (178.28)	180	180	180	180	180

[a] Experimental values in parentheses are from ref 52.

TABLE 2: The Computed Dipole Polarizabilities (1×10^{-24} esu) for Systems 1−6

system	α_{xx}	α_{yy}	α_{zz}	$\langle\alpha\rangle$
1	70.92	57.65	198.54	109.03
2	72.65	58.27	315.18	148.69
3	71.82	58.48	202.33	110.88
4	82.94	63.60	419.00	188.51
5	88.61	66.35	435.44	196.79
6	87.64	65.10	452.34	201.70

Triple-ζ plus polarization basis sets were used to describe the valence electrons of all atoms, whereas for the transition metal molybdenum atom, a frozen core composed of 1s to 3spd shells was described by means of single Slater functions. In calculations of the polarizability, second-order polarizability, and excitation property, the RESPONSE and EXCITATION modules[43] implemented in the ADF program were used based on the optimized geometries. The van Leeuwen−Baerends XC potential (LB94) was chosen for calculations of all the response properties.[44] The reliability of LB94 potential to calculate polarizabilites and hyperpolarizabilities has already been proven and well-documented.[36,45−47] The adiabatic local density approximation (ALDA) was applied for the evaluation of the first and second functional derivatives of the XC potential. Moreover, the value of the numerical integration parameter used to determine the precision of numerical integrals was 6.0. The change of dipole moment between ground and excited states ($\Delta\mu$) has been calculated from the field dependence of the excitation energies by using the TDDFT method as implemented in ADF.[48] GaussSum[49] was used to calculate density of states (DOS). The functional and basis set choices for our studied inorganic−organic hybrid compounds were based on the research work which has already been reported.[33,38,50,51]

3. Molecular Structures

The geometrical optimization of all systems (**1**−**6**) under symmetry constraint C_{2v} was carried out, where as initial geometric data were obtained from the crystal data.[52] Their structures are sketched in Figure 1 and the optimized bond distances are given in Table 1, which are in reasonable agreement with reported experimental data.

All the systems from **1** to **6** investigated here show C_{2v} symmetry. The symmetry axis is along the *z*-axis. Moreover, by using TDDFT our group has already studied some experimental cases close to organoimido hexamolybdates derivatives in which the calculated electronic absorption spectra have shown good consistency with experimental data.[38,53] As far as Scheme 1 is concerned, it shows the hypothetical calculation models with sketch map of various D−A configurations of studied systems.

4. Results and Discussion

4.1. Dipole Polarizability. For the discussion of the second-order polarizability (β), examining the physical mechanism concerning determination of the dipole polarizability (α) is also important. The average polarizability, $\langle\alpha\rangle$ is given by

$$\langle\alpha\rangle = 1/3(\alpha_{xx} + \alpha_{yy} + \alpha_{zz}) \quad (1)$$

The computed dipole polarizability coefficients for systems **1**−**6** are listed in Table 2. Due to the C_{2v} symmetry of the studied systems, only the diagonal dipole polarizability tensors α_{ii} ($i = x, y, z$) are nonzero. Among the α_{ii} components, the α_{zz} component is the largest, while the α_{xx} and α_{yy} components are smaller. Hence, the property of the studied compounds (**1**−**6**) is dominantly determined by the *z*-direction transition (Figure 1). The expression of dipole polarizability (*z*-direction) is described in the following equation

$$\alpha_{zz} \propto \frac{(M_z^{gm})^2}{E_{gm}} \quad (2)$$

According to eq 2, we can know that the α value is directly proportional to the square of transition moment and is inversely proportional to the transition energy. As a result, the system with a strong electronic absorption peak will have a larger α value. Transition wavelengths (λ_{gm}), transition moment (M_z^{gm}), and corresponding dominant molecular orbital (MO) transitions of systems **1**−**6** are provided in Table 3. The average polarizability, $\langle\alpha\rangle$ is in the following order: system **6** > **5** >**4** > **2** > **3** > **1** as shown in Table 2.

According to the TDDFT calculations, the electron transition of system **1** mainly arises from polyanion (HOMO) to organoimido segment (LUMO+2) and (HOMO-2) to (LUMO+2) along the *z*-direction, and this character of charge transfer similarly occurs on system **2** (HOMO to LUMO), system **3** (HOMO to LUMO+2), system **4** (HOMO-1 to LUMO), (HOMO-5 to LUMO) and system **5** (HOMO-1 to LUMO), (HOMO-5 to LUMO). The molecular orbitals involved in the dominant electron transitions in systems **1**−**5** are shown in Figure 2. The electronic transition of system **6** is more interesting as it originates not only from polyanion (HOMO-2 and HOMO-7) but also from amino group (HOMO-11) to organoimido segment (LUMO). The molecular orbitals involved in the dominant electron transitions in system **6** are shown in Figure 3.

Under the C_{2v} symmetry constraints, electronic transitions from the ground state to the singlet A_1 (*z*-direction) excited states are electric dipole allowed for our studied systems. For present calculated systems (**1**−**6**), the dominant electron transitions have A_1 symmetry (see Table 3).

Although the changes of molecular structures modify the contribution of different orbitals to the electronic transitions, the dominant electron transitions for the studied compounds have the same A_1 symmetry; that is, the major charge transfer originates from polyanion to organic/organoimido segment along the *z*-axis. These behaviors indicate that the organoimido segment acts as an acceptor and polyanion acts as a donor, which is different from the character of charge transfer for arylimido hexamolybdates derivatives.[33] In system **1** polyanion is acting as a donor while organoimido is behaving as an acceptor through its conjugated bridge (see Figure 2). The charge transfer in system **2** is from polyanion toward nitro group ($-NO_2$) via a conjugated bridge of organoimido segment. In system **3** the amino group ($-NH_2$), a strong donor at the end of organoimido segment competes with polyanion (D) as a result of which

SCHEME 1: Hypothetical calculation Models with Sketch Map of Various D−A Configurations of POMs

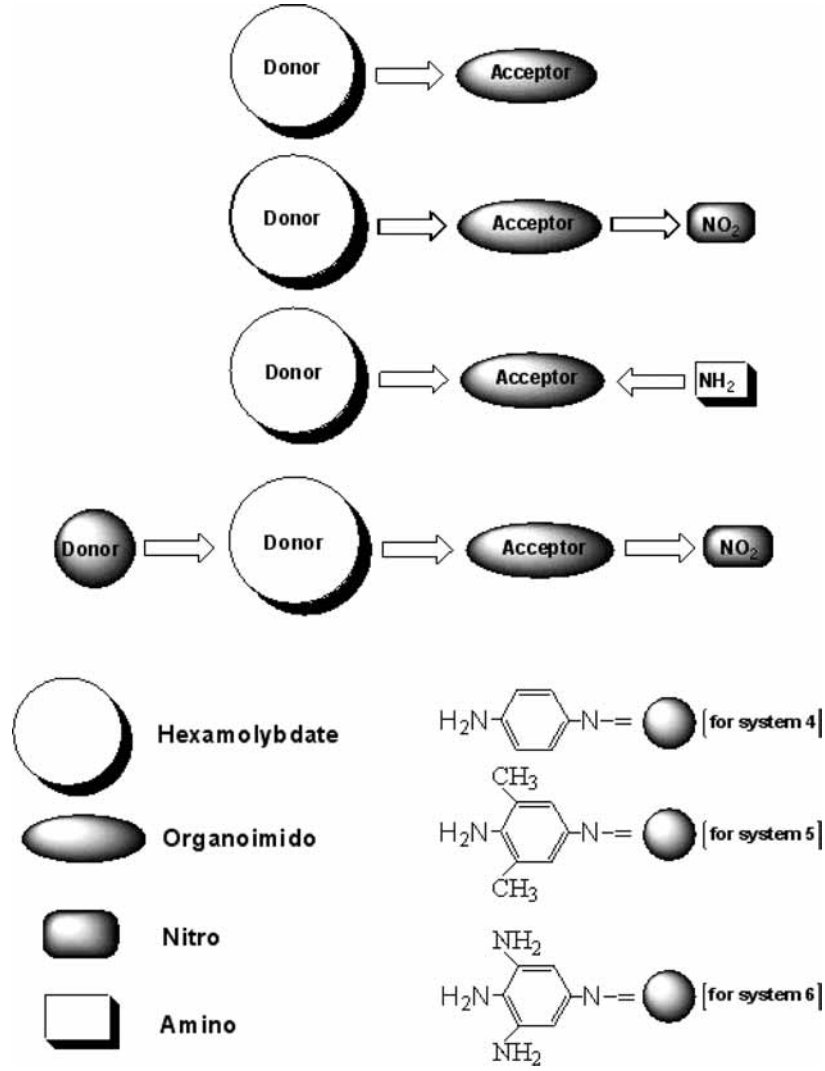

TABLE 3: Excitation Energy (λ_{gm}, nm; E, a.u.), Difference in Dipole Moment ($\Delta\mu$, a.u.)[a] Oscillator Strengths (f), Symmetry (S), Transition Moment (M_z^{gm}, a.u.),[b] and Corresponding Dominant MO Transitions of Systems 1−6

system	λ_{gm}	$\Delta\mu$	f	E	S	M_z^{gm}	MO transition
1	554	3.9	0.8568	0.0822	A_1	3.9545	HOMO → LUMO+2 (74%) HOMO-2 → LUMO+2 (11%)
2	807	1.1	1.0329	0.0564	A_1	5.2392	HOMO → LUMO (77%) HOMO-2 → LUMO (7%)
3	533	1.6	0.9276	0.0854	A_1	4.0354	HOMO → LUMO+2 (74%)
4	810	1.3	1.1901	0.0562	A_1	5.6383	HOMO-1 → LUMO (76%) HOMO-5 → LUMO (13%)
5	810	1.3	1.2477	0.0562	A_1	5.7692	HOMO-1 → LUMO (76%) HOMO-5 → LUMO (13%)
6	818	1.0	1.0181	0.0558	A_1	5.2325	HOMO-2 → LUMO (59%) HOMO-11→ LUMO (14%) HOMO-7 → LUMO (11%)

[a] Calculated from the field dependence.[48] [b] $M_x^{ng} = M_y^{ng} = 0$.

pattern of charge transfer is somewhat localized in the center of organic segment as shown in Figure 2. The systems **4**, **5**, and**6** prove that the organoimido segment acts as an acceptor and conjugated bridge as well when amino ($-NH_2$) is introduced at the outer side of polyanion (D) ring.

The bonding behavior between organoimido and $[Mo_6O_{19}]^{2-}$ has already been studied,[32] and the results show that the strong Mo≡N triple bond can be formed through the N → Mo σ-donation, N → Mo π-donation (from occupied orbital of organoimido into the empty d_{z^2} orbital of Mo), and N → Mo π-back-donation (from the d_{xz} and d_{yz} orbitals of Mo to the empty N p-orbital of organoimido) in the formation of the organoimido derivative. This strong interaction in terms of σ-overlap and π-overlap generates a strong electronic communication between organoimido and $[Mo_6O_{19}]^{2-}$. As shown in Table 3, the lowest energy electronic absorptions are significantly red-shifted from parent $[Mo_6O_{19}]^{2-}$ (the calculated value is 313 nm whereas the experimental value is 325 nm)[38]

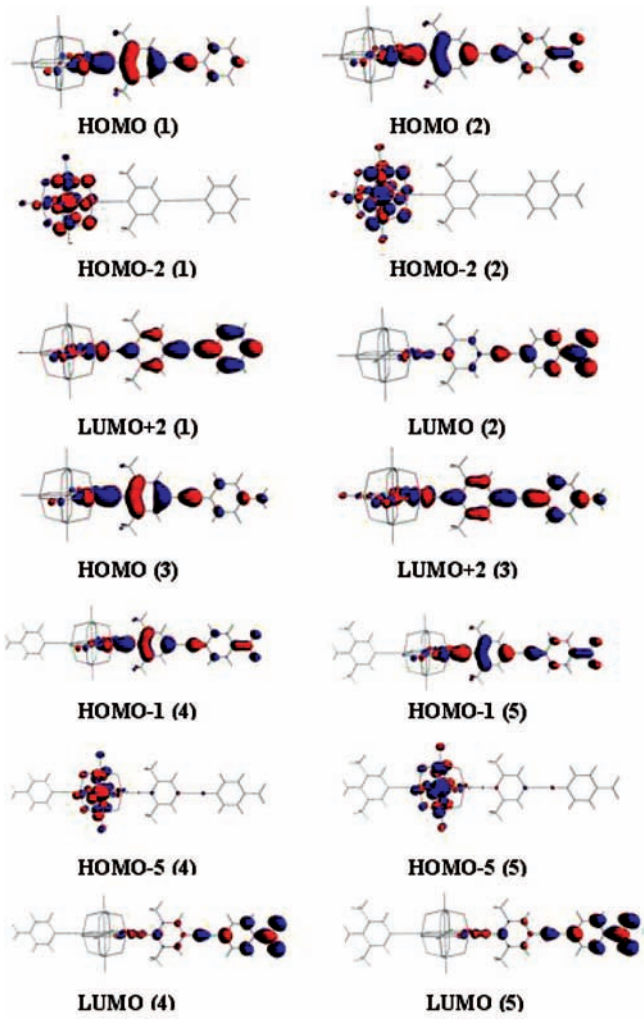

Figure 2. The frontier molecular orbitals of systems **1**−**5** involved in the dominant electron transitions.

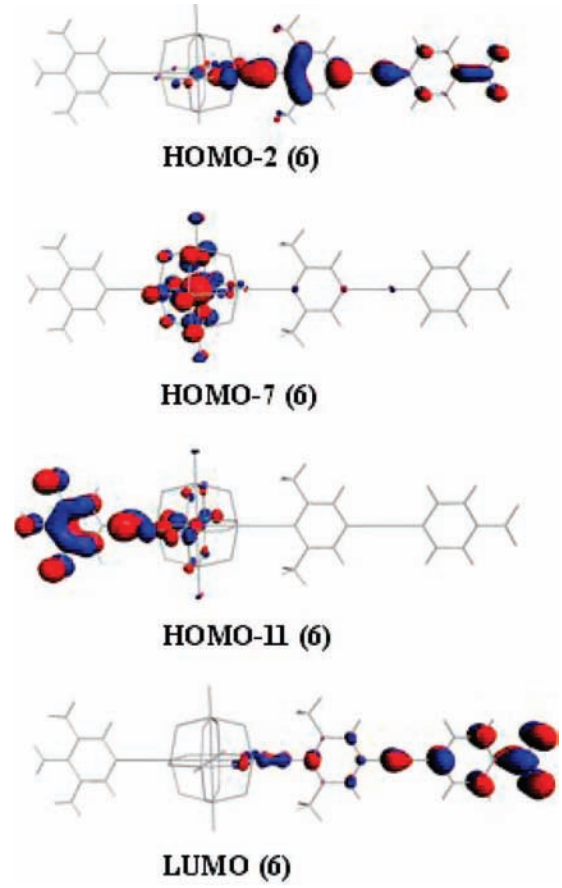

Figure 3. The frontier molecular orbitals of system **6** involved in the dominant electron transitions.

to studied systems (**1**−**6**). If, as commonly believed, the lowest energy absorption is due to the charge-transfer transition that originated in a state dominated by Mo−N π-bonding,[15] the bathochromic shifts observed may imply that the Mo−N π-bond is delocalized with the organic conjugated π-electrons. In other words, there is a strong electronic interaction between the metal−oxygen cluster and the organic segment. In our systems (**1**−**6**) conjugation of π-electrons between two phenyl rings has been enhanced with the presence of the C≡C triple bond; the C−C π-bond along with the Mo−N π-bond is delocalized with the conjugation of two phenyl rings. Thus π-conjugation is extended and the delocalization is further improved from system **1** to system **2** by introducing an electron acceptor (the nitro group). This extended conjugation leads to smaller transition energy which increases the degree of charge transfer. Therefore a large β_{vec} value has been generated in system **2** as compared to system**1**. The conjugation has been further extended in systems **4**, **5**, and **6** which leads to smaller transition energy and greater degree of charge transfer as shown in Figure 3. In frontier molecular orbitals of systems **1**−**6**, polyanion can modify the occupied molecular orbitals and extend its conjugation of π-electrons to the end phenyl ring in organoimido segment as shown in Figures 2 and 3 which results in charge transfer (CT) from polyanion to organoimido segment.

4.2. Static Second-Order Polarizability. The second-order polarizability is related to second-harmonic generation (SHG). For these polyanions with their dipole moment along the *z*-axis, β_{vec} is given by

$$\beta_{vec} = \frac{1}{3}\sum_{i=x,y,z}(\beta_{zii} + \beta_{izi} + \beta_{iiz}) \qquad (3)$$

The static second-order polarizability (β_{vec}) is termed as the zero-frequency hyperpolarizability and is an estimate of the intrinsic molecular hyperpolarizability in the absence of resonance effect. The computed β_{vec} values and its individual components of systems **1**−**6** are shown in Table 4. There are seven components of the second-order polarizability owing to the C_{2v} symmetry. As the discussion in the dipole polarizability, the β_{zzz} component has the largest value. Hence, the major contribution to the second-order polarizability is the β_{zzz} component and the major charge transfer is also along the *z*-direction. As shown in Table 4, all systems have larger second-order polarizability coefficients. For example, the computed β_{vec} value of system **4** is about 14827 times larger than the average second-order polarizability of the organic urea molecule[54] and 329 times larger than measured value for highly π-delocalized phenyliminomethyl ferrocene complex.[55] This indicates that all the studied systems except system **3** (see Table 4) have an excellent second-order NLO response. In system **3** (D−A−D configuration), the transition can be assigned to the CT from HOMO to LUMO+2. Here, the NH_2 competes with polyanion due to electron-donating ability of both NH_2 and polyanion; the CT pattern is somewhat localized in center leading to minimal NLO response.

TABLE 4: Computed Static Second-Order Polarizabilities and Their Individual Components (1×10^{-30} esu) for Systems 1−6

system	β_{zzz}	β_{yyz}	β_{xxz}	β_{yzy}	β_{zyy}	β_{xzx}	β_{zxx}	β_{vec}
1	351.520	1.125	0.892	1.125	1.125	0.892	0.892	212.146
2	−700.770	1.650	3.022	1.650	1.650	3.022	3.022	419.679
3	−182.690	−0.831	−2.510	−0.831	−0.831	−2.510	−2.510	111.628
4	2364.600	−0.976	5.813	−0.976	−0.976	5.813	5.813	1416.009
5	−3648.600	−0.031	7.254	−0.031	−0.031	7.254	7.254	2182.440
6	−10499.000	−0.197	−0.952	−0.197	−0.197	0.952	0.952	6299.596

Due to charge transfer along the z-axis in systems **1**−**6** the computed β_{vec} values of these systems show that the NLO response is as follows: system **6** > **5** > **4** > **2** > **1** > **3**. The β_{zzz} component of system **2** is greater than that of system **1** due to presence of a nitro group which established D−A−A configuration, the β_{zzz} component of system **4** is greater than that of system **2** due to having D−D−A−A configuration, whereas system **3** (D−A−D) shows the least β_{zzz} and β_{vec} values due to insignificant charge transfer (CT) and greater transition energy (2.3250 eV) (see Figures 2 and 4). The β_{zzz} component of system **6** has the highest value as it shows the largest β_{vec} from systems **1**−**6**.

However, the β_{vec} values of systems **4** and **2** are seven times and two times larger than that of system **1**, respectively, whereas system **3** is half of system **1**. In system **2**, the donating effect of polyanion has been enhanced by incorporation of electron acceptor ($-NO_2$) at the end of phenyl ring while this effect is further enhanced by introducing an electron donor ($-NH_2$) at the outer side of polyanion in system **4**. As for system **5**, it has significantly high NLO response as donating ability of the NH_2 group (attached at the outer side of polyanion in systems **4** and**5** having DDAA configuration) has been amplified by incorporating two methyl ($-CH_3$) groups sidewise as shown in Figure 1. In system **5** the two CH_3 groups at the outer side of polyanion along with the NH_2 group enhance the donating ability of polyanion, so the β_{vec} value has been increased from 1416.00 $\times 10^{-30}$ esu (system **4**) to 2182.44 $\times 10^{-30}$ esu (system **5**). The system **6** has maximal NLO response among all six systems as donating ability of polyanion has been enhanced by incorporating three amino groups at the outer side of polyanion ring which further supports our idea/conclusion that substitution of amino group ($-NH_2$) at the outer side of polyanion and an electron acceptor ($-NO_2$) at the end phenyl ring in organoimido segment simultaneously is more important to enhance the optical nonlinearity, the system **6** is the state-of-the-art with regard to systems **4** and **5** as it shows highest NLO response among all studied systems (**1**−**6**) by establishing D−D−A−A configuration which validates our idea that polyanion is acting as a donor in our all studied systems. The degree of charge transfer and synergistic effect between polyanion (D) and organoimido segment (conjugated bridge) have been remarkably enhanced by introducing three amino groups ($-NH_2$) at the outer side of polyanion ring (see system **6**). The NLO properties of our studied systems have been improved remarkably through the increase of the conjugation path and the choice of donors/acceptor. Particularly, for our studied organic−inorganic hybrid materials, their NLO properties have been ameliorated through the introduction of the donors at the outer side of the polyanion ring, this incorporation of donor is helpful to enhance the degree of charge transfer by decreasing the excited energy which leads to remarkable increase in the first hyperpolarizability as it is much pronounced in system **6** where the β_{vec} value is computed to be 6299.59 $\times 10^{-30}$ esu. (See Figure 3 and Table 3.)

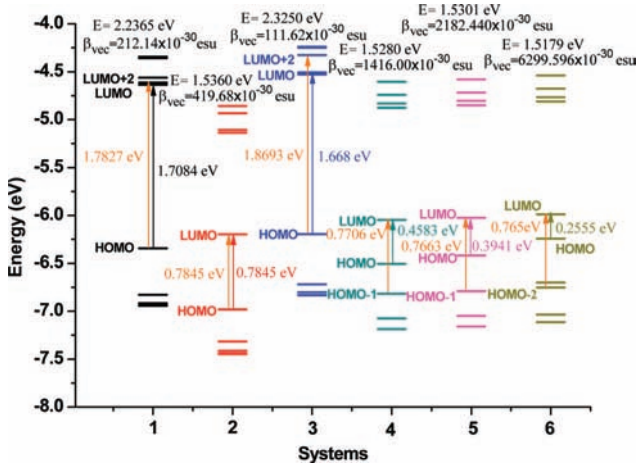

Figure 4. Molecular orbital diagram, transition energy (E), oscillator strength (f), and arrows indicate HOMO−LUMO and major MO transition energy gaps (orange font) of systems **1**−**6**.

To throw further light on the origin of second-order NLO properties of the studied compounds, the demonstration of structure−property relationship is mandatory. How does it cause the variations in the computed β_{vec} values? From the complex sum-over-states (SOS) expression, the two-state model that linked between β and a low-lying charge transfer transition has been established.[56] For the static case, the following model expression is employed to estimate β_{CT}

$$\beta_{CT} \propto \frac{\Delta\mu_{gm} f_{gm}}{E_{gm}^{3}} \tag{4}$$

where f_{gm}, E_{gm}, and $\Delta\mu_{gm}$ are the oscillator strength, the transition energy, and the difference of the dipole moment between the ground state (g) and the mth excited state (m), respectively. In the two-state model expression, the second-order polarizability caused by charge transfer, β_{CT}, is proportional to the optical intensity and is inversely proportional to the cube of the transition energy. Therefore, for any noncentrosymmetric molecule, the low transition energy (<1 au) is the decisive factor for the large β. Hence, for the studied compounds, the low excitation energy is the decisive factor in the β value. As can be found from Table 3, the λ_{gm} values are related to the structural character of the studied compounds. The computed M_z^{gm} values of systems **2**, **4**, **5**, and **6** are comparable; however, the λ_{gm} values increase as follows; system **1** < **2** < **4** = **5** < **6**. The λ_{gm} value of system **1** is only 554 nm, whereas it is large for system **4** and **5** (810 nm), a bit larger for system **6** (818 nm). The bathochromic shift of the absorption band attributes the substitution of a donor and acceptor. From eq 4, this behavior significantly enhances β_{vec} value. Distinctly, the excitation energy will tend to make dominant contribution to the β_{vec} values of the studied compounds. As we have already demonstrated that the β value is directly proportional to oscillator strength and $\Delta\mu$ (the difference of the dipole moment between the ground state and the excited state) while inversely proportional to the

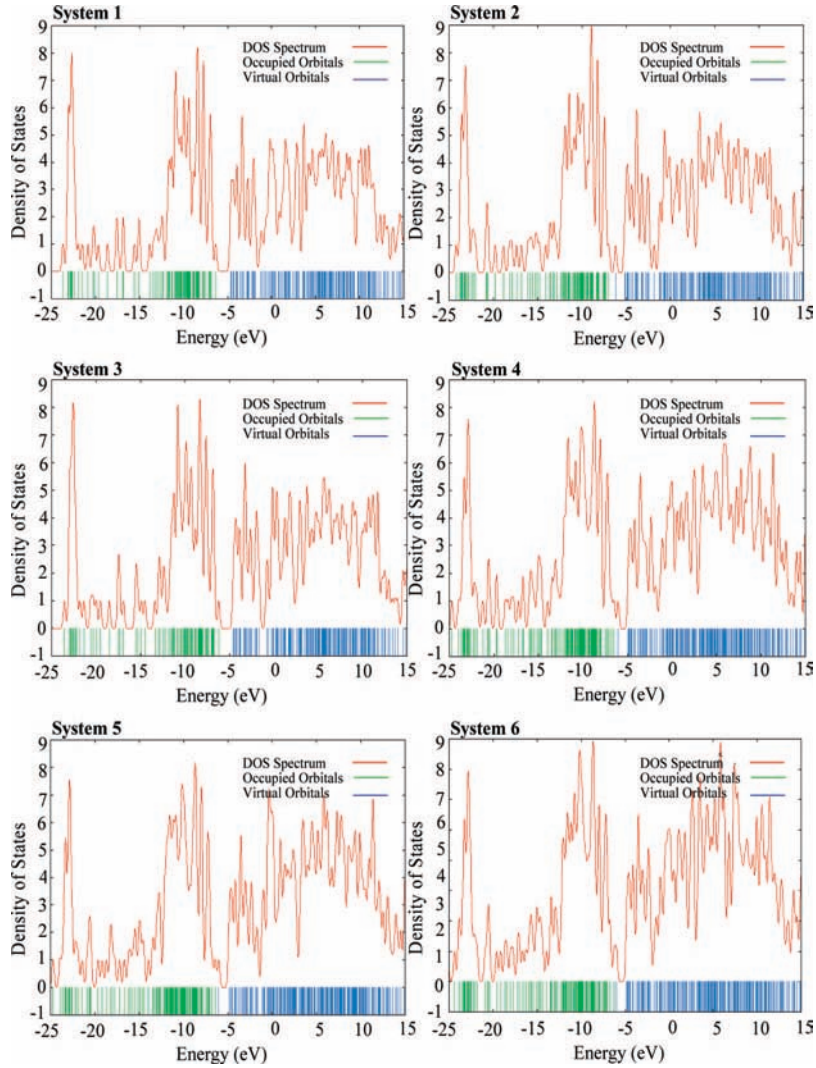

Figure 5. Calculated DOS spectra for systems**1**−**6**.

transition energy. The low excitation energy is the decisive factor in the β value as it has been observed in systems **1**−**6** that low lying transition energy is a decisive/conclusive factor to determine NLO response as shown in Table 3. However, the oscillator strength f_{gm} for systems **1**−**6** are 0.8568, 1.0329, 0.9276, 1.1901 1.2477, and 1.0181, respectively. The values of difference in $\Delta\mu$ (in a.u.) for systems **1**−**6** are 3.9, 1.1, 1.6, 1.3, 1.3, and 1.0 a.u., respectively (see Table 3). Systems **4** and **5** have exactly same difference in $\Delta\mu$ (1.3 a.u.) and same transition energy (0.0562 a.u.) while oscillator strength of system **5** is greater than that in system **4**, which is also a key factor as it has power to assign NLO response while comparing both of these systems. The systems **4**, **5**, and **6** possess the identical conjugation bridge, which is why they have not much difference in $\Delta\mu$. Therefore, in these systems low-lying excitation energy is the principle factor for increasing the β_{vec} value.

In a nut shell, the large β_{vec} values come from the strong oscillator strength and small transition energy as shown in Table 3. So, the NLO response of systems **1**−**6** is as follows: system **6** > **5** > **4** > **2** > **1** > **3** and it is obvious that system **6** is offering maximum β value by establishing D−D−A−A configuration/relationship. It is also crystal clear that substitution of donor and acceptor has a majestic influence on the second-order NLO property in our studied systems. From these results, it can be concluded that incorporation of an electron donor/donors at the outer side of polyanion and an electron acceptor at the end

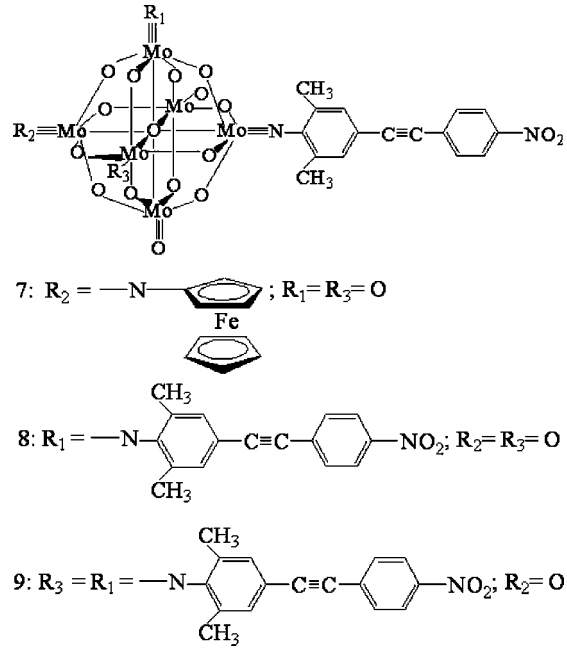

Figure 6. Calculation models for systems **7**−**9**.

phenyl ring of organoimido segment simultaneously is helpful to enhance the β value. In systems **1**−**6**, another important factor

SCHEME 2: Hypothetical Calculation Models with Sketch Map of D−D−A−A, 2D, and 3D Configurations of POMs

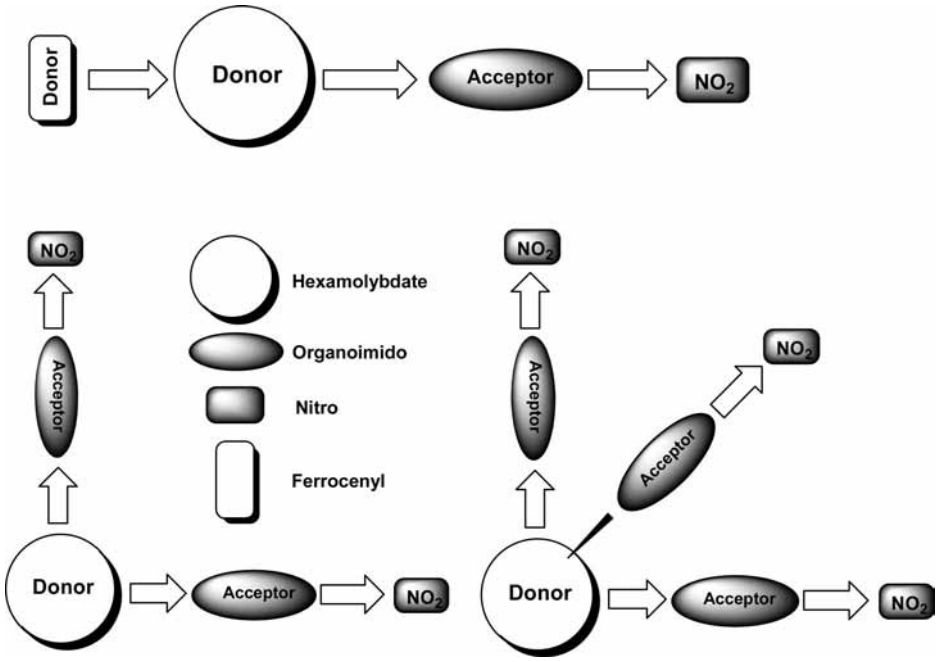

is lengthening via C≡C; thus the π-conjugation is extended and the delocalization is improved and introduction of donor and acceptor at the same time in systems **4**, **5**, and **6** enhances the β_{vec} value, more extended conjugation generally leads to a smaller energy difference between the ground and charge transfer excited states and, accordingly enhance the degree of charge transfer. Therefore, the larger β_{vec} values are generated, as electron transition originates from polyanion to organic segment along the *z*-axis. It is well-known that second-order NLO property is governed by the values of the transition moments and the transition energy. In systems **1**−**6** the transition moments are in following order: system **6** > **5** > **4** > **2** > **3** > **1**. The HOMO−LUMO gaps of systems **1** and **3** are comparable, but transition energy of system **3** is greater than that of system **1** which leads to minimal NLO response of system **3** as the β value is inversely proportional to the transition energy. Generally, the HOMO−LUMO gap is decreased by introduction of an electron-withdrawing group (−NO_2) as occurred in systems **2**, **4**, **5**, and **6**. As for the HOMO−LUMO energy gaps of systems **1**−**6**, it can be seen in Figure 4 that the HOMO−LUMO energy gap of system **6** has the least value of 0.2555 eV.

The low-lying HOMO−LUMO gap might enhance molecular second-order NLO properties. The energy gaps of major molecular orbital transitions are decreasing in the following order: system **3** > **1** > **2** > **4** > **5** > **6** while the NLO response is increasing accordingly as follows: system **3** < **1** < **2** < **4** < **5** < **6**. The HOMO−LUMO energy gaps and MO transition energy gaps of systems **1**−**6** are decreasing almost in same sequence (see Figure 4), It means system **6** has a least energy gap giving rise to maximal NLO response among all studied compounds as shown in Figure 4.

4.3. Density of States Calculation. Density of states (DOS) calculations have been carried out by using GaussSum,[49] it was used to convolute density of states spectra from the molecular orbital data for systems **1**−**6**. The density of states in a band could be very large for some materials, it may not be uniform. It approaches zero at the band boundaries and is generally highest near the middle of a band as its corresponding in our studied systems (see Figure 5). The investigated systems are particularly interesting for the nonlinear optical properties, appropriately operating by the substitution of donors and acceptor. Due to appropriate changes of the systems, one can also vary the NLO properties. Thus one requires reliable information about band structure which could be gathered from DOS diagram. We present results of the band structure and DOS for systems **1**−**6** as nonlinear optical compounds. We have for the first time performed the investigations of the electronic density of the states for inorganic−organic hybrid (organoimido derivatives of hexamolybdates) compounds. We have found that the system with smallest band gap (E_g) possesses maximal NLO response (system **6** with band gap 0.25 eV). This band gap is one of the most useful aspects of the band structure, as it strongly influences the electrical and optical properties of the material. Electrons can be transferred from one band to the other by means of carrier generation and recombination processes. The band gap and defect states created in the band gap by doping can be used to create devices in materials science such as solar cells, diodes, transistors, laser diodes, and others. DOS spectra are in good accord with the NLO response of our studied systems as the system with smallest band gap (energy gap) possesses maximal NLO response. So investigations of their band structure may play a principal role in understanding their physical properties (NLO).

To study the density of states, band structure (BS) may help to further study the nonlinear optical (NLO) applications. According to DOS spectra diagrams, band gap is decreasing as size of molecule is increasing from system **1** to **6** as shown in Figure 5. In general, the band gap decreases with increasing molecular size.[57] This low-lying band gap might enhance second-order NLO response, which is in good agreement with our studied systems. The band gap is decreasing from systems **1** to **2**, **2** to **4**, **4** to **5**, and then**5** to**6**. NLO response is increasing as follows: system **1** < **2** < **4** < **5** < **6**. With the increase of conjugation, band gap is decreasing from system **1** to **6** as shown in DOS diagram, this low-lying band gap leads to bathochromic shift (red shift) in systems **2**, **4**, **5**, and **6** while system **3** is blue-shifted compared to system **1** as shown in Table 3 and Figure 5. The values of band gaps in systems **1**−**6** are 1.70, 0.78, 1.66,

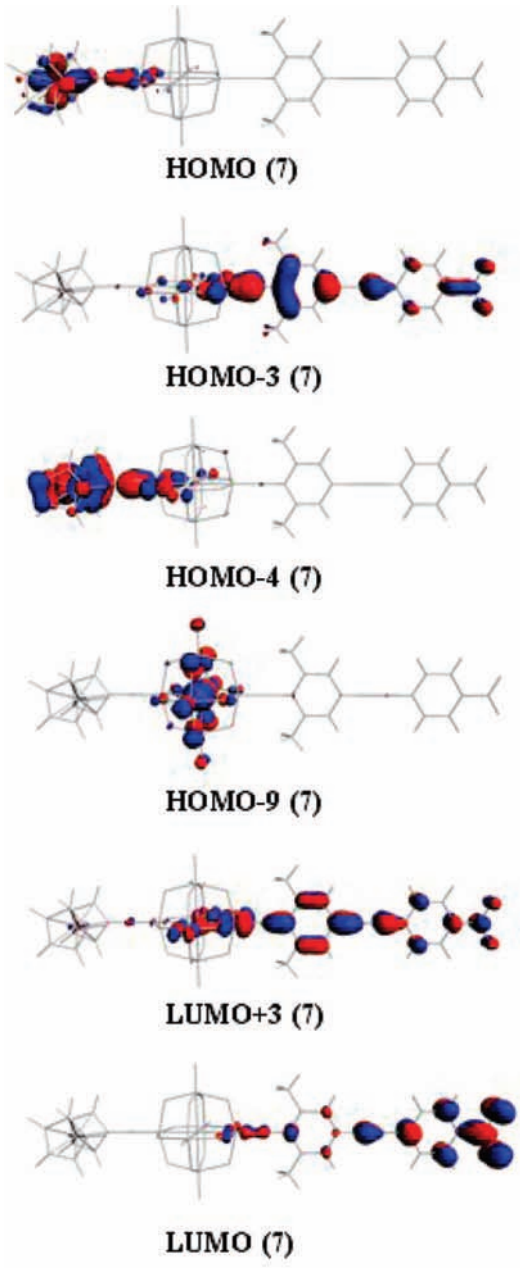

Figure 7. The frontier molecular orbitals of system **7** involved in the dominant electron transitions.

0.45, 0.39, and 0.25 eV, respectively, which are significantly reduced as compared to parent $[Mo_6O_{19}]^{2-}$ ($E_g = 2.68$ eV).[58] It is well-known that a material with a small, but not null or negative, band gap (arbitrarily defined as <3 eV) is referred to as a semiconductor; band gaps of our studied systems are less than 3 eV, so these might be good candidates for semiconductors. Moreover, the valence band is concentrating near the Fermi level as we move from system **1** to **6** (see Figure 5). The band gaps of systems **4**, **5**, and **6** are reduced remarkably due to incorporation of electron-donating groups. This interesting DOS study may evoke a potential chance for the experimentalists to make NLO materials with remarkably large NLO response and unique molecular semiconductors or conductors as well based on POM−organic hybrid materials.

On the basis of the special character of charge transfer and the large β_{zzz} value of systems **1**−**6**, we were inspired to probe into the role of a different but powerful donor at the outer side of the polyanion ring and the effect of more than one electron-acceptor groups ($-NO_2$) in influencing the NLO response so we have also studied systems **7** (D−D−A−A), **8** (2D), and **9** (3D) as shown in Figure 6 and Scheme 2.

In system **7**, we have incorporated ferrocenyl donor at the outer side of polyanion ring, and the choice of introducing ferrocenyl ligand as a strong donor was based on previous experimental work.[59] In system **7**, donating ability of polyanion has been remarkably enhanced and the β_{vec} value was computed to be 15766.27×10^{-30} esu, which is the result of the existence of charge-transfer transition from polyanion and ferrocenyl donor to organoimido segment along the *z*-direction leading to exceptionally and remarkably large NLO response among all the studied systems as shown in Figure 7 and Table 5.

The systems **7** and **8** investigated here show C1 and C_{2v} symmetry while symmetry axes are along the *z*-axis and the bisector of the *y*- and *z*-axes, respectively, whereas system **9** has no symmetry. Moreover, the charge transfer in system **8** arises from (HOMO-1 → LUMO), (HOMO → LUMO+1), and (HOMO-7 → LUMO+1) and this character of charge transfer similarly occurs on system **9** (HOMO-4 → LUMO).

The molecular orbitals involved in the dominant electron transitions in systems **8** and **9** are shown in Figures 8 and 9, respectively.

The calculated β_{vec} values of systems **8** and **9** are 674.18×10^{-30} and 1079.22×10^{-30} esu, respectively. For system **8**, the main contribution of β_{vec} is in the *y* and *z* directions, so β_{yyz}, β_{yzy}, and β_{zyy} components have larger values than those of the other tensors. This point is in accord with the direction of the charge transfer (see Figure 8), In system **9** the main contribution of β_{vec} is in all three *x*, *y*, and *z* directions so β_{yyy}, $\beta_{xyy,}$ β_{yxy}, $\beta_{yyx,}$ β_{yzz}, $\beta_{zyz,}$ β_{zzy}, β_{zxz}, and β_{zzx} components have larger values among 27 tensors; this point is also in accord with the direction of the charge transfer (see Figure 9). Theoretically, we have constructed and investigated systems **7**, **8**, and **9** with donor−donor−acceptor−acceptor (D−D−A−A), two-dimensional (2D), and three-dimensional (3D) characteristics, respectively. The system **7** is a masterpiece of D−D−A−A structural configuration by showing the outstanding and maximal NLO response

TABLE 5: Symmetry (S), Transition Moments (M_x^{gm}, M_y^{gm}, M_z^{gm}, a.u.), the β_{zzz} Components, Computed Static Second-Order Polarizabilities (1×10^{-30} esu), and Corresponding Dominant MO Transitions for Systems 7−9

system	S	M_x^{gm}	M_y^{gm}	M_z^{gm}	β_{zzz}	β_{vec}	MO transition
7 (DDAA)	A	0.0695	0.2484	5.0209	−26242.000	15766.272	HOMO-3 → LUMO (63%) HOMO-9 → LUMO (11%) HOMO→ LUMO+3 (11%) HOMO-4→ LUMO (3%)
8 (2D)	A_1	0.0000	0.0000	4.0080	−373.910	674.187	HOMO-1 → LUMO (31%) HOMO→ LUMO+1 (29%) HOMO-7→ LUMO+1 (28%)
9 (3D)	A	0.0961	2.2403	3.6821	146.210	1079.222	HOMO-4 → LUMO (18%)

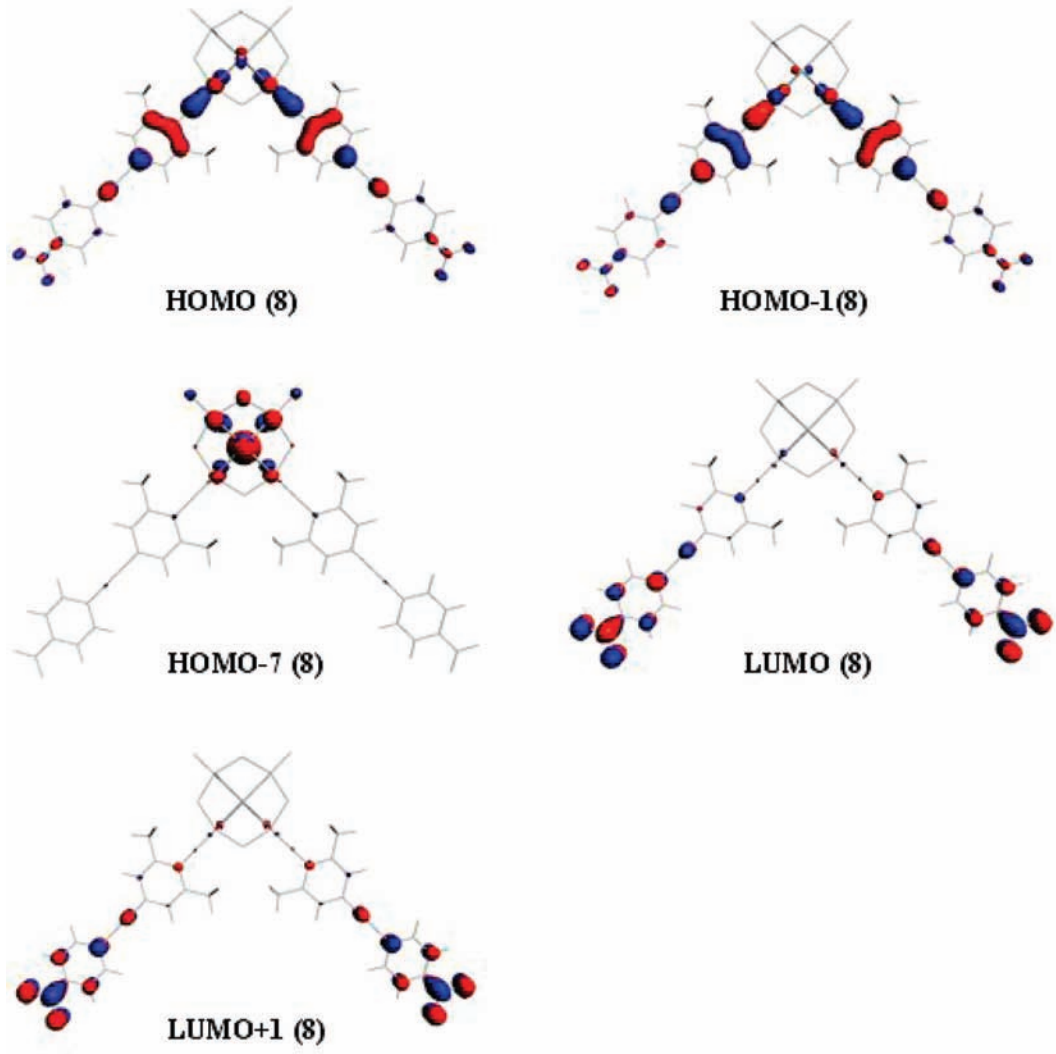

Figure 8. The frontier molecular orbitals of system **8** involved in the dominant electron transitions.

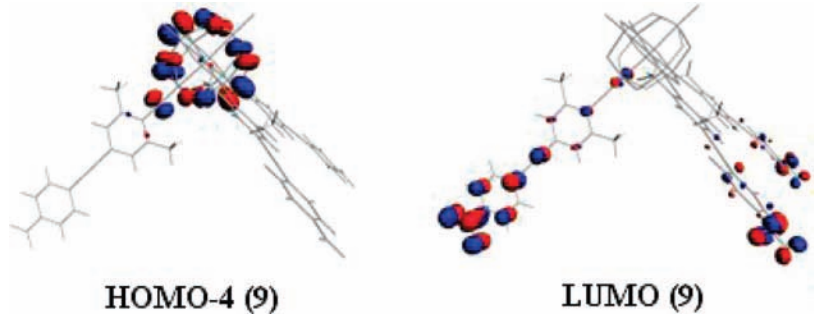

Figure 9. The frontier molecular orbitals of system **9** involved in the dominant electron transitions.

among all the studied systems (**1**−**9**) whereas the static second-order polarizability (β_{vec}) is distinctly enhanced in 2D and 3D compounds. The β_{vec} values of 2D and 3D are comparatively larger than their parent system **2**, with regard to transparency/efficiency tradeoff, and superior to system **2** because a major drawback of conventional 1D NLO materials is the so-called nonlinearity/transparency tradeoff. Further studies on NLO properties of 2D and 3D organoimido polyanions by DFT method are in progress. The present investigation gives insight into the NLO properties of organoimido polyanion and attempts to reveal the origin of the remarkably large NLO properties of this family of hybrid compounds, which are interesting and appealing in design and synthesis of new promising NLO material. For our studied systems, the incorporation of an electron acceptor (the nitro group) leads to a larger β value, while introduction of an electron donor (the amino group or ferrocenyl ligand) at the outer side of polyanion and an electron acceptor at the end phenyl ring of organoimido segment leads to remarkably large and eye-catching β values. These POM-based organic−inorganic hybrid compounds can become an excellent kind of material in the second-order NLO field. The electron acceptor in the organoimido segment enhances the first hyperpolarizability whereas the electron donor in the organoimido ligand reduces the first hyperpolarizability in our studied systems as the polyanion acts as a donor and the organoimido ligand acts as an acceptor.

The present DFT calculations predict the β_{vec} values of systems **8** and **9** are 674.18×10^{-30} and 1079.22×10^{-30} esu, respectively. It is noticeable that systems **8** and**9** have the same geometrical character as the *p*-nitroaniline. It forms a dipolar molecule containing an electron-donor group connected to an electron acceptor via a π-conjugated bridge, in which π-conjugation commonly provides a pathway for the redistribution of electrons under the influence of an electric field.[60] In the *p*-nitroaniline, the charge transfer occurs between the nitryl and the benzene. Under the laser frequency of $\omega = 0.65$ eV, the β value of *p*-nitroaniline is 9.2×10^{-30} esu in experiments[61] and 11.28×10^{-30} esu in present DFT calculations. While the β value of *p*-nitroaniline is computed to be 8.9×10^{-30} esu at the static electronic field. The computed β_{vec} value of system **8** is about 75 times and for system **9** is about 121 times larger than the static second-order polarizability of *p*-nitroaniline. Therefore, the larger β_{vec} values are generated, as electron transition originates from polyanion to organoimido segment.

5. Conclusions

Organoimido-substituted hexamolybdates are found to possess considerably large static second-order polarizabilities. Systems with an electron donor ($-NH_2$ or $-FeC_{10}H_9$) and an electron acceptor ($-NO_2$) at the same time have remarkably large static second-order polarizabilities. The optical excitation analysis in terms of frontier MOs shows that the charge transfer from polyanion to organic segment plays the key role in the NLO response. In systems **1**−**7** CT from polyanion to the organic segment along the *z*-axis is a vital determinant for the NLO response. According to the two-state model, the low excitation energy is the decisive factor in the large β value. Compounds with the transition of longer wavelength have a higher computed β value. In the framework of this theoretical study, we can conclude the following points: (1) The structure−property relationship indicates that there are several ways to enhance the NLO response of this class of compounds. (2) The incorporation of an electron acceptor ($-NO_2$) at the end of phenyl ring leads to a larger β value by establishing D−A−A configuration. (3) The incorporation of an electron donor ($-NH_2$) at the outer side of polyanion and electron acceptor ($-NO_2$) at the end phenyl ring in organoimido segment simultaneously lead to a remarkably large β value by establishing D−D−A−A relationship and this configuration is strongly validated by system **6** in which donating ability of a polyanion has been considerably enhanced as compared to systems **4** and **5**. This is also the most important point to increase the optical nonlinearity. (4) The substitution of an electron donor ($-NH_2$) at the end of organoimido segment as in system **3** leads to the least β value due to insignificant charge transfer and larger value of transition energy. (5) System **7** is a masterpiece of D−D−A−A structural configuration by showing the maximal NLO response among all the studied systems. (6) Systems **8** and **9** with 2D and 3D characteristics, respectively, are found to possess considerably large β values due to two-dimensional and three-dimensional CT which is helpful to improve the nonlinearity/transparency tradeoff. (7) These POM-based organic−inorganic molecules can become an excellent kind of material in the second-order NLO field. The present calculations on organoimido derivatives of hexamolybdates provide the theoretical framework in which the charge transfer and NLO properties may be understood. The polyanion-to-organoimido charge transfer may be responsible for the NLO properties of this kind of compounds. This work exhibits the tunable NLO behavior of organoimido hexamolybdates and may provide new ways for the experimentalists to design high-performance NLO materials.

Acknowledgment. The authors gratefully acknowledge the financial support from the National Natural Science Foundation of China (Project No. 20573016) and Program for Changjiang Scholars and Innovative Research Team in University (IRT0714). Muhammad Ramzan Saeed Ashraf Janjua acknowledges the Government of Pakistan (Ministry of Education) and Chinese Scholarship Council for the award of a PhD scholarship. Janjua is also thankful to Maheen Gull, Saira Janjua, and Sareb Janjua for their support and cooperation. We thank Yuhe Kan for computational assistance.

References and Notes

(1) Pope, M. T. *Heteropoly and Isopoly Oxometalates*; Springer-Verlag: New York, 1983.
(2) Hill, C. L. *Chem. Rev.* **1998**, *98*, 1.
(3) Pope, M. L.; Müller, A. *Angew. Chem., Int. Ed. Engl.* **1991**, *30*, 34.
(4) Hill, C. L.; Prosser-McCarther, C. M. *Coord. Chem. Rev.* **1995**, *143*, 407.
(5) Baker, L. C. W.; Figgis, J. S. *J. Am. Chem. Soc.* **1970**, *92*, 3794.
(6) Zeng, H.; Newkome, G. R.; Hill, C. T. *Angew. Chem., Int. Ed.* **2000**, *39*, 1771.
(7) Gouzerh, P.; Proust, A. *Chem. Rev.* **1998**, *98*, 77.
(8) Du, Y.; Rheingold, A. L.; Maatta, E. A. *J. Am. Chem. Soc.* **1992**, *114*, 346.
(9) Clegg, W.; Errington, R. J.; Fraser, K.; Holmes, S. A.; Schäfer, A. *J. Chem. Soc., Chem. Commun.* **1995**, 455.
(10) Proust, A.; Thouvenot, R.; Chaussade, M.; Robert, F.; Gouzerh, P. *Inorg. Chim. Acta* **1994**, *224*, 81.
(11) Wei, Y. G.; Xu, B. B.; Barnes, C. L.; Peng, Z. H. *J. Am. Chem. Soc.* **2001**, *123*, 4083.
(12) Wei, Y. G.; Lu, M.; Cheung, C. F.-C.; Barnes, C. L.; Peng, Z. H. *Inorg. Chem.* **2001**, *40*, 5489.
(13) Xu, L.; Lu, M.; Xu, B. B.; Wei, Y. G.; Peng, Z. H.; Powell, D. R. *Angew. Chem., Int. Ed.* **2002**, *41*, 4129.
(14) Judeinstein, P. *Chem. Mater.* **1992**, *4*, 4.
(15) Strong, J. B.; Yap, G. P. A.; Ostrander, R.; Liable-Sands, L. M.; Rheingold, A. L.; Thouvenot, R.; Gouzerh, P.; Maatta, E. A. *J. Am. Chem. Soc.* **2000**, *122*, 639.
(16) (a) Mayer, C. R.; Cabuil, V.; Lalot, T.; Thouvenot, R. *Angew. Chem.* **1999**, *111*, 3878. (b) Mayer, C. R.; Cabuil, V.; Lalot, T.; Thouvenot, R. *Angew. Chem., Int. Ed.* **1999**, *38*, 3672.
(17) Mayer, C. R.; Thouvenot, R.; Lalot, T. *Chem. Mater.* **2000**, *12*, 57.
(18) Schroden, R. C.; Blanford, C. F.; Melde, B. J.; Johnson, B. J. S.; Stein, A. *Chem. Mater.* **2001**, *13*, 1074.
(19) Johnson, B. J. S.; Stein, A. *Inorg. Chem.* **2001**, *40*, 801.
(20) Strong, J. B.; Haggerty, B. S.; Rheingold, A. L.; Maatta, E. A. *Chem. Commun.* **1997**, 1137.
(21) Moore, A. R.; Kwen, H.; Beatty, A. B.; Maatta, E. A. *Chem. Commun.* **2000**, 1793.
(22) Xu, B. B.; Wei, Y. G.; Barnes, C. L.; Peng, Z. H. *Angew. Chem., Int. Ed.* **2001**, *40*, 2290.
(23) Lu, M.; Wei, Y. G.; Xu, B. B.; Cheung, C. F. C.; Peng, Z. H.; Powell, D. R. *Angew. Chem., Int. Ed.* **2001**, *41*, 1566.
(24) (a) Pope, M. T. *Heteropoly and Isopoly Oxometalates*; Springer-Verlag: Berlin, 1983. (b) Pope, M. T.; Müller, A. *Polyoxometalates: From Platonic Solid to Anti-Retroviral Activity*; Kluwer: Dordrecht, 1994. (c) Rhule, J. T.; Hill, C. L.; Judd, D. A. *Chem. Rev.* **1998**, *98*, 327. (d) Hasenknopf, B. *Front. Biosci.* **2005**, *10*, 275. (e) Yin, C. X.; Sasaki, Y.; Finke, R. G. *Inorg. Chem.* **2005**, *44*, 8521. (f) Gong, Y.; Hu, C. W.; Liang, H. *Front. Biosci.* **2005**, *15*, 385. (g) Proust, A. *Actual. Chim.* **2000**, *7*−*8*, 55. (h) Casañ-Pastor, N.; Gomez-Romero, P. *Front. Biosci.* **2004**, *9*, 1759.
(25) Gouzerh, P.; Proust, A. *Chem. Rev.* **1998**, *98*, 77.
(26) Coronado, E.; Gómez-García, C. J. *Chem. Rev.* **1998**, *98*, 273.
(27) Blau, W. *Phys. Technol.* **1987**, *18*, 250.
(28) Nie, W. *Adv. Mater.* **1993**, *5*, 520.
(29) Powell, C. E.; Humphrey, M. G. *Coord. Chem. Rev.* **2004**, *248*, 725.
(30) Bredas, J. L.; Adant, C.; Tackx, P.; Persoons, A.; Persoons, B. M. *Chem. Rev.* **1994**, *94*, 243.
(31) Katsoulis, D. E. *Chem. Rev.* **1998**, *98*, 359.
(32) Yan, L. K.; Su, Z. M.; Guan, W.; Zhang, M.; Chen, G. H.; Xu, L.; Wang, E. B. *J. Phys. Chem. B* **2004**, *108*, 17337.

(33) Yan, L. K.; Yang, G. C.; Guan, W.; Su, Z. M.; Wang, R. S. *J. Phys. Chem. B* **2005**, *109*, 22332.

(34) Bredas, J. L.; Beljonne, D.; Coropceanu, V.; Cornil, J. *Chem. Rev.* **2004**, *104*, 4971.

(35) Locknar, S. A.; Peteanu, L. A.; Shuai, Z. G. *J. Phys. Chem. A* **1999**, *103*, 2197.

(36) van Gisbergen, S. J. A.; Snijders, J. G.; Baerends, E. J. *J. Chem. Phys.* **1998**, *109* (24), 10644.

(37) (a) Rohmer, M. M.; Bénard, M.; Blaudeau, J. P.; Maestre, J. M.; Poblet, J. M *Coord. Chem. Rev.* **1998**, *178*−*180*, 1019. (b) Lopez, X.; Bo, C.; Poblet, J. M. *J. Am. Chem. Soc.* **2002**, *124*, 12574. (c) Bridgeman, A. J.; Cavigliasso, G. *Inorg. Chem.* **2002**, *41*, 3500.

(38) Yang, G. C.; Guan, W.; Yan, L. K.; Su, Z. M.; Xu, L.; Wang, E. B. *J. Phys. Chem. B* **2006**, *110*, 23092.

(39) (a) te Velde, G.; Bickelhaupt, F. M.; Baerends, E. J.; Fonseca Guerra, C.; van Gisbergen, S. J. A.; Snijders, J. G.; Ziegler, T. Chemistry with ADF. *J. Comput. Chem.* **2001**, *22*, 931. (b) Fonseca Guerra, C.; Snijders, J. G.; Te Velde, G.; Baerends, E. J. *Theor. Chem. Acc.* **1998**, *99*, 391. (c) ADF2006.01, SCM, Theoretical Chemistry, Vrije Universiteit, Amsterdam, The Netherlands, http://www.scm.com.

(40) van Lenthe, E.; Baerends, E. J.; Snijders, J. G. *J. Chem. Phys.* **1993**, *99*, 4597.

(41) Becke, A. D. *Phys. Rev. A* **1988**, *38*, 3098.

(42) Perdew, J. P. *Phys. Rev. B* **1986**, *33*, 8822.

(43) van Gisbergen, S. J. A.; Snijders, J. G.; Baerends, E. J. *Comput. Phys. Commun.* **1999**, *118*, 119.

(44) van Leeuwen, R.; Baerends, E. J. *Phys. Rev. A* **1994**, *49*, 2421.

(45) van Gisbergen, S. J. A.; Osinga, V. P.; Gritsenko, O. V.; van Leeuwen, R.; Snijders, J. G.; Baerends, E. J. *J. Chem. Phys.* **1996**, *105* (7), 3142.

(46) van Gisbergen, S. J. A.; Snijders, J. G.; Baerends, E. J. *J. Chem. Phys. Rev. Lett.* **1997**, *78*, 3097.

(47) van Gisbergen, S. J. A.; Snijders, J. G.; Baerends, E. J. *J. Chem. Phys.* **1998**, *109*, 10657.

(48) Grozema, F. C.; Telesca, R.; Jonkman, H. T.; Siebbeles, L. D. A.; Snijders, J. G. *J. Chem. Phys.* **2001**, *115*, 10014.

(49) O'Boyle, N. M.; Tenderholt, A. L.; Langner, K. M. *J. Comput. Chem.* **2008**, *29*, 839.

(50) (a) Guan, W.; Yang, G. C.; Yan, L. K.; Su, Z. M. *Inorg. Chem.* **2006**, *45*, 7864. (b) Guan, W.; Yang, G. C.; Yan, L. K.; Su, Z. M. *Eur. J. Inorg. Chem.* **2006**, *20*, 4179.

(51) Carey, D. M-L.; Munoz-Castro, A.; Bustos, C. J.; Manriquez, J. M.; Arratia-Perez, R *J. Phys. Chem. A* **2007**, *111*, 6563.

(52) (a) Lu, M.; Wei, Y, G.; Xu, B, B.; Cheung, C, F, C.; Peng, Z, H; Powell, D, R. *Angew. Chem., Int. Ed.* **2002**, *41*, 1566. (b) Xu, B. B.; Wei, Y. G.; Barnes, C. L.; Peng, Z. H. *Angew. Chem., Int. Ed.* **2001**, *40* (12), 2290.

(53) Yan, L. K.; Jin, M. S.; Zhuang, J.; Liu, C. G.; Su, Z. M.; Sun, C. C *J. Phys. Chem. A* **2008**, *112*, 9919.

(54) Kanis, D. R.; Ratner, M. A.; Marks, T. J. *Chem. Rev.* **1994**, *94*, 195.

(55) Pal, S. K.; Krishnan, A.; Das, P. K.; Samnelson, A. G. *J. Organomet. Chem.* **2000**, *604*, 248.

(56) (a) Oudar, J. L.; Chemla, D. S. *J. Chem. Phys.* **1977**, *66*, 2664. (b) Oudar, J. L. *J. Chem. Phys.* **1977**, *67*, 446.

(57) Haberlen, O. D.; Chung, S.-C.; Stener, M.; Rosch, N. *J. Chem. Phys.* **1997**, *106*, 5189.

(58) Xia, Y.; Wu, P.; Wei, Y.; Wang, Y.; Guo, H. *Cryst. Growth Des.* **2006**, *6*, 253.

(59) Stark, J, L.; Young, V, G.; Maatta, E, A *Angew. Chem., Int. Ed.* **1995**, *107*, 2751.

(60) Rao, V. P.; Jen, A. K.-Y.; Chandrasekhar, J.; Namboothiri, I. N. N.; Rathna, A. *J. Am. Chem. Soc.* **1996**, *118*, 12443.

(61) Cheng, L.; Tam, W.; Stevenson, S. H.; Meredith, G. R.; Rikken, G.; Marder, S. R. *J. Phys. Chem.* **1991**, *95*, 10631.

JP808707Q